

Acoustic Wave Propagation in Water Filled Buried Polyethylene Pipes

T. Graf*, T. Gisler, P. Sollberger and O. Schälli
School of Engineering and Architecture,
Lucerne University, Technikumstrasse 21, CH-6048 Horw, Switzerland
*Corresponding author: thomas.graf@hslu.ch

Abstract: Axisymmetric acoustic wave-modes propagating along buried water pipes have been investigated by the method of finite elements and experimentally. High precision dispersion relations are presented in this paper as a function of the geometry, the embedding material and the elastic modulus of the pipes.

It is found that at low frequencies the fundamental axisymmetric acoustic mode of the water cylinder is nearly a plane wave. This mode is the dominant component of a leak noise signal propagating along the pipe. At moderate frequencies the acoustic pressure is small in the centre of the water column and builds up close to the wall of the pipe, inside and outside the elastic pipe layer. Attenuation at moderate frequencies is not substantial. At high frequencies an additional mode emerges in the water cylinder, driven by the wave in the elastic pipe wall.

Keywords: Buried polyethylene water pipes, leak detection, axisymmetric acoustic mode, acoustic phase velocity, finite element modeling (FEM).

1. Introduction

It is difficult to perceive leaks in the water distribution pipework at an early stage, and even more difficult to pinpoint the source of the leak. The former is of great importance for minimizing water losses, the latter is important for taking efficient repair action.

The company Hinni AG [1] is the leading manufacturer of hydrants in Switzerland. In 2005 Hinni AG introduced a monitoring system of the water usage which can distinguish water leaks. Their method is based on hydrants which are equipped with hydrophones. The hydrophones are situated close to the pipe flow. The noise of the water flow is recorded periodically. The monitoring system can identify a leak in the pipe network as distinct deviations of the background noise [2].

Together with Hinni AG we are currently establishing a method to also locate the source of the leak. The technique relies on the acoustic

noise recorded at two hydrant sites. The time delay of the cross-correlated acoustic signals yields a length difference of the guiding pipe sections and thus pinpoints the leak. Details of this detection method can be found in Refs. [3-6]. In order to locate the leak precisely detailed knowledge of the noise propagation is essential. Dispersion and attenuation of the acoustic wave and scattering at joints, fittings and bends blur the correlation function and render the task of localization very difficult.

In Switzerland the water supply system is mapped and the pipe distance between hydrants can be determined accurately. The dimensions and the materials of pipes for drinking water are standardized and known in the distribution net. The water supply is largely ensured by iron pipes. Yet new sections of the supply system are often built with plastic pipes. With these figures it is in principle possible to calculate the phase velocities of the acoustic signal propagating along different sections of the distribution system.

Guided waves in buried water pipes have been studied in the past. Long et al. determined dispersion curves and attenuation for axisymmetric modes in water filled iron pipes [6, 7]. The authors developed their own modelling program DISPERSE. The program is based on partial wave analysis in the different material layers. The wave directions and complex amplitudes are resolved iteratively to satisfy the boundary conditions. Long et al. employed Bessel functions to model the partial waves in cylindrical layers.

Muggleton et al. [8] used an analytical approach for the wave propagation in water-filled, buried plastic pipes. They described the acoustic pressure waves in the water cylinder by a sum of Bessel functions. The waves in the soil consisted of a set of Hankel functions for the outgoing longitudinal pressure wave and the outgoing shear wave. Their analysis is restricted to low frequencies and includes some simplifications.

Baik et al [9] computed dispersion and attenuation curves for waves propagating in

liquid-filled elastic tubes in vacuum. The authors equated Bessel functions at the boundaries of the different media and solved the corresponding equations numerically.

We opted for a strait forward and practical approach to characterize the noise propagation in buried pipes. We computed the solutions of the governing field equations in different media and various frequencies by the method of finite elements (FEM) and compared the results with experiments. No a priori wave functions were assumed.

In section 2. we describe the finite element model, including the governing equations and the boundary conditions. In section 3. we explain the experimental setup. The numerical simulation results are discussed and validated in section 4. We conclude our analysis in section 5.

2. FEM Model

FEM computations were performed using the *Acoustic-Structure Interaction Module* of COMSOL Multiphysics® [10]. The pipe is treated as an elastic layer, the water in the pipe and the surrounding soil or air are modelled as fluids. The program solves two coupled equations. The elastic wave equation for the displacement field \vec{u} is solved in the pipe layer:

$$\frac{\partial^2 \vec{u}}{\partial t^2} - c_1^2 \nabla (\nabla \cdot \vec{u}) + c_2^2 \nabla \times (\nabla \times \vec{u}) = 0 \quad (1)$$

The quantities c_1 and c_2 are defined by:

$$c_1^2 = \frac{\lambda_L + 2\mu_L}{\rho} \quad \text{and} \quad c_2^2 = \frac{\mu_L}{\rho}, \quad \text{where } \lambda_L \text{ and } \mu_L$$

are the Lamé constants in Pa and ρ is the material density in kg/m³. ρ is independent of position.

Simultaneously the acoustic wave equation or Helmholtz equation for the pressure field p is solved in the fluids:

$$\nabla \left(\frac{1}{\rho} \nabla p \right) - \frac{1}{\rho c^2} \frac{\partial^2 p}{\partial t^2} = 0 \quad (2)$$

where c is the sound velocity in m/s and ρ is the fluid density in kg/m³. The boundary conditions for the fluid - elastic layer interaction are given by the equations:

$$-\vec{n} \frac{1}{\rho} \nabla p = \vec{n} \frac{\partial^2 \vec{u}}{\partial t^2} \quad \text{and} \quad \underline{\underline{\sigma}} \cdot \vec{n} = p \vec{n} \quad (3)$$

where \vec{n} is the unit vector perpendicular to the elastic layer and $\underline{\underline{\sigma}}$ is the stress tensor in the elastic material. The two equations of Eq. (3) correspond to Newton's law and to the continuity of the normal stress component through the elastic layer, respectively. For details of the theory of elastic and acoustic waves see classical textbooks, e.g. Ref. [11]. The second time derivatives in Eqs. (1), (2) and (3) are replaced by the factor $-\omega^2$ in the *Frequency Domain Study* and the *Eigenfrequency Study*, where ω is the angular frequency in rad/s.

The acoustic wave propagation along various polyethylene pipes is computed for a 2D axisymmetric geometry (see Fig. 1.). Typical values of the material parameters used in the simulations are given in table 1. In the *Frequency Domain Study* the acoustic wave was excited at one end of the water cylinder by a *Normal Acceleration* boundary condition ($a_n = 0.1 \text{m/s}^2$).

3. Experimental Setup

The cross-correlation method described in the introduction and in Refs. [3-6] was examined in long (up to 200 m), buried pipe sections of the public water supply network. The technique allowed for the detection of test leaks (e.g. an open hydrant between two hydrophones) with a position accuracy of better than 1 m, if the signal velocity was known precisely (e.g. by separate measurements or by means of simulations).

Phase velocities were measured in a separate experiment (see Fig. 2.). A polyethylene pipe of 131 mm bore diameter was filled with water under 8 bar of pressure. The pipe was held in air. A pseudo-random white noise signal was generated at one end of the pipe. Two hydrophones were plugged into the pipe, 11 m apart. The signals captured by the hydrophones were read simultaneously by high-fidelity audio preamplifiers and ADCs. The recorded signals were then further processed with the program Matlab® [13], yielding the impulse response, the frequency response and the phase velocities in the 11 m pipe section. The phase velocities can be determined very accurately in the polyethylene test pipe between 40 and 800 Hz.

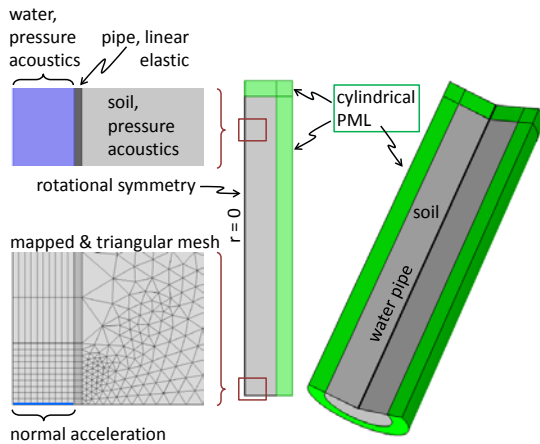


Figure 1. Axisymmetric setup of the FEM model. At low frequencies elongated domains were necessary to analyze at least half a wavelength along the pipe. A structured mesh was implemented to keep the number of nodes moderate.



Figure 2. Part of the test bench to measure phase velocities in water pipes. A public hydrant fills the pipe with water by means of a fire hose (on the left). A loudspeaker box encloses the 8 bar-pressurized hose and generates the white noise signal (center). The signal propagates along the pipe on the right.

Table 1. Material properties used in the FEM simulations. The values of polyethylene PE100 are taken from Ref. [12]

Material	Property	Value
Water, 20°C	Density ρ	1000 kg/m ³
	Speed of sound c	1481 m/s
Soil	Density ρ	2500 kg/m ³
	Speed of sound c	1000 m/s
Air, 20°C	Density ρ	1.19 kg/m ³
	Speed of sound c	343 m/s
Polyethylene (PE100)	Density ρ	950 kg/m ³
	Elastic modulus E	1.1×10^9 Pa
	Poisson's ratio ν	0.33

4. Numerical Simulation Results

In most studies accelerometers are used to detect leak noise. The accelerometers are

attached to the stem of a hydrant or to the pipe. Yet the hydrants of Hinni AG are equipped with hydrophones [2], allowing for detection of the signal directly in the water column.

We investigated primarily the fundamental mode of the water column inside the pipe, often called the α_1 mode in the literature (e.g. Ref. [6]). In subsection 4.1 we present the dispersion relations of this mode as a function of the pipe geometry, the pipe elasticity and the surrounding material. We then discuss higher modes and show their cut-on frequencies as a function of the elastic modulus of the pipe wall in subsection 4.2.

4.1 Fundamental α_1 Mode in Water Column

An important characteristics of polyethylene pipes is the *standard dimension ratio* of the outer diameter D to the wall thickness T , labeled $SDR = D/T$. Pipes for drinking water are produced in a variety of diameters but commonly in only two SDR categories, namely 11 and 17.

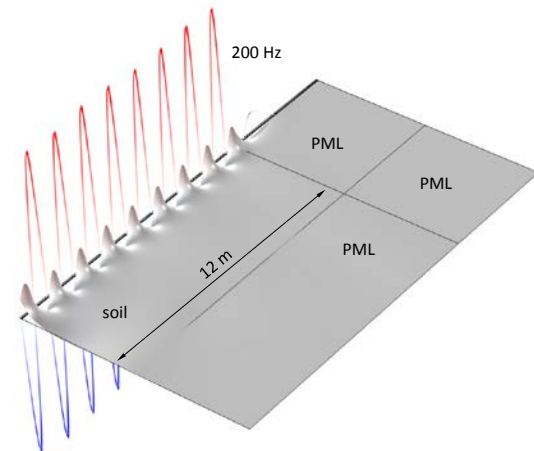


Figure 3. Simulated acoustic pressure wave in a straight, axisymmetric water-pipe-soil section. The wave is excited harmonically with 200 Hz in the far left corner of the domain. The acoustic pressure builds up at the pipe wall. A large-amplitude wave (red and blue oscillations) propagates in the water column, a small-amplitude wave propagates in the soil adherent to the pipe. Note the phase shift of half a wavelength between the wave in the water and in the soil, reminiscent to the radial displacement of the pipe layer. The simulation domains are terminated by perfectly matched layers (PML). Hardly any radiation loss can be detected in the soil.

Figure 3 shows an example of a simulated acoustic wave in a water-pipe-soil domain. The outer diameter of the pipe is $D = 160$ mm and the wall thickness is $T = 14.6$ mm (\Rightarrow SDR 11). Inspection of the computed wave inside the water column yields the wavelength of the $\alpha 1$ mode. The wavelength multiplied by the exciting frequency determines the phase velocity for this particular frequency. For example a phase velocity of $v = 287$ m/s is obtained from Fig. 3.

The result of numerous simulations and calculations is compiled in figure 4. as a function of various pipe diameters. Note that the elastic modulus was set to $E = 2.2$ GPa, twice as much as given by the pipe manufacturer (compare to table 1.). The choice of $E = 2.2$ GPa is suggested by validation measurements (see below). The different curves of Fig. 4. are merely frequency-shifted. This simple shift allows for scaling, yielding a universal curve for a particular SDR, independent of the pipe diameter. The norm frequency and the relative frequency are defined as:

$$f_{norm} = c_w / d\pi$$

$$f_{rel} = \frac{f}{f_{norm}} = \frac{f \cdot d\pi}{c_w} \quad (4)$$

where d is the bore diameter of the pipe and c_w is the bulk sound velocity of water (see table 1.).

Fig. 5. displays the sound velocity as a function of relative frequency. Each data point in the figure corresponds to a simulation for a specific diameter of the pipe and a particular pipe surrounding. Inspection of Fig. 5. reveals that at low frequency the phase velocity of the sound in the water column depends on the SDR (and the E -modulus), but not on the pipe surrounding material, i.e. soil or air. In contrast at high frequency the phase velocity of the $\alpha 1$ mode in the pipe is strongly coupled to the wave propagation in the substance embedding the pipe, but is not dependent on the SDR. It is also visible in Fig. 5. that at low relative frequency there is little dispersion and the curves are almost horizontal. Little dispersion of the phase velocity and minor dependence on the embedding material are two preferred features for the cross correlation technique mentioned above.

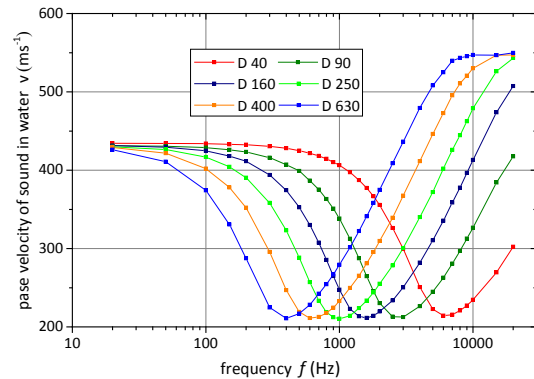


Figure 4. Calculated phase velocity v of the fundamental acoustic $\alpha 1$ mode in polyethylene pipes as a function of frequency f . The pipes are buried in soil. The different curves correspond to different outer diameters D in mm. The pipe characteristics are: elastic modulus $E = 2.2$ GPa, density $\rho = 0.95$ g/cm³, ratio of outer diameter to wall thickness SDR = 11.

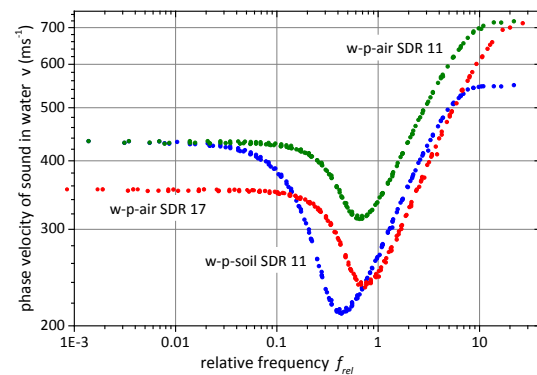


Figure 5. Calculated phase velocity v of the acoustic $\alpha 1$ mode in polyethylene pipes ($E = 2.2$ GPa, $\rho = 0.95$ g/cm³) as a function of relative frequency. The three curves correspond to different SDR ratios and different material surrounding the pipe. Each curve comprises data of various pipe diameters as in Fig. 4.

Figure 6. shows the phase velocity versus the frequency for varying pipe elasticity. The pipes were surrounded by air in order to compare the numerical results with experiments. At small E -modulus of the pipe wall the v vs. f curve exhibits a distinct velocity dip. At large E -modulus (hard wall), the dip disappears and evolves into a velocity step. In hard pipes (large E) the phase velocity at high frequency becomes that of the bulk sound velocity in water (1481 m/s, table 1.).

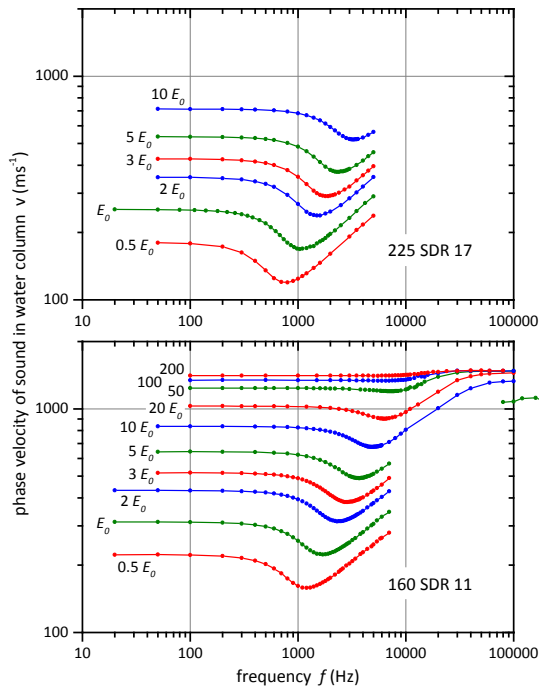


Figure 6. Phase velocity v of the acoustic α_1 mode in polyethylene pipes as a function of frequency f . The different curves correspond to different multiples of the elastic modulus $E_0 = 1.1$ GPa (Ref. [12]). The upper graph displays data of a pipe with 225 mm outer diameter and 13.4 mm wall thickness (SDR 17), the lower graph data of a pipe with 160 mm outer diameter and 14.6 mm wall thickness (SDR 11). The pipes are surrounded by air.

The curves of Fig. 6. are compared to experiments in Fig. 7. There exists excellent agreement between the measurement and the simulation with $E = 2.2$ GPa. The E -modulus of the pipe material was determined in a separate experiment. Small beams of rectangular shape were cut from polyethylene pipes. The free oscillation periods of various beams were measured and the E -modulus could thus be calculated. By this method we determined an elastic modulus for the pipe material of 1.6 ± 0.1 GPa. This value is smaller than 2.2 GPa for the perfect match in Fig. 7., but definitely larger than 1.1 GPa given by the manufacturer (e.g. Ref [12]). In order to find an explanation for these discrepancies the following facts ought to be considered. First the pipes are under 8 bar water pressure during the phase velocity experiments, rendering the pipe wall possibly

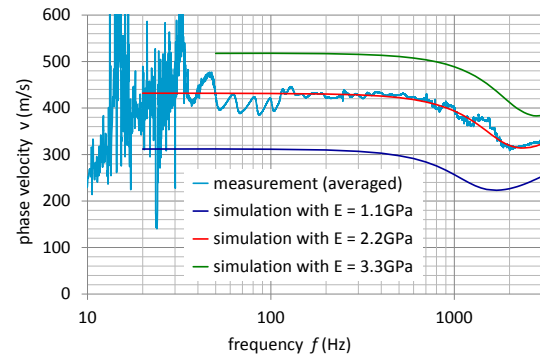


Figure 7. Phase velocity v of the acoustic α_1 mode in polyethylene pipes as a function of frequency f . The outer diameter of the pipe is 160 mm and the wall thickness is 14.6 mm (SDR 11). The pipe was surrounded by air. The wiggly curve is experimental data according to Sect. 3., the straight lines are simulations for three different elastic moduli.

stiffer than the wall of empty pipes. Second the outside layer of the pipe wall cools faster than the layer inside during the pipe casting process, causing prestress in the pipe wall. The observed distortion of the cut beams is reminiscent of the stress in the pipe wall. Third the oscillations of beams of the pipe material are probably not harmonic but comprise plastic deformation. The beams do not relax completely after oscillation experiments. For practical applications and with regard to leak detection in pressurized polyethylene pipes the phase velocity of water can be modelled accurately with $E = 2.2$ GPa. The density of the polyethylene pipe, given in table 1. could be confirmed exactly with a simple water displacement experiment.

Fig. 8. displays characteristic parameters of the curves in Fig. 6. as a function of the elastic modulus E , namely: the low frequency velocity v_0 (“DC velocity”), the minimum velocity v_{\min} of the various curves and the frequency f_{\min} (lower graph), at which this minimum velocity occurs. In hard pipes with large E the velocities v_0 and v_{\min} converge, the velocity minimum evolves into a velocity step and f_{\min} approaches zero. For the leak detection by the cross-correlation method v_0 is the essential parameter. v_0 is often equated to the assumed non-dispersive leak noise propagation velocity v_{NDLN} . An estimate of v_{NDLN} can be found in the literature (e.g. Ref. [6]):

$$v_{NDLN} = \frac{c_w}{\sqrt{1 + \frac{B_w \cdot d}{E \cdot T}}} = \frac{c_w}{\sqrt{1 + \frac{B_w}{E} (SDR - 2)}} \quad (5)$$

where c_w is the bulk sound velocity of water, d is the inner diameter of the pipe, T is the wall thickness of the pipe and, B_w is the bulk modulus of water, E is the elastic modulus of the pipe material and SDR is the standard dimension ratio $D/T = (d+2T)/T$, where D is the outer diameter. Figure 8. illustrates that v_0 and v_{NDLN} are in perfect agreement, if the bulk modulus is $B_w = 2.5$ GPa. This value is somewhat larger than $B_w = 2.2$ GPa commonly used for water. With the common B_w value Eq. (5) overestimates the low frequency phase velocity v_0 by about 5%.

4.2 Eigenmodes and Cut-Off Frequency

Eigenfrequency analyses were performed on water-pipe cross sections in 2D geometry. The pipes were surrounded by vacuum (or air). The program COMSOL found a great number of different eigenfrequencies and eigenmodes. The smaller the elastic E modulus of the pipe wall the more eigenfrequencies were found. Only axisymmetric modes were relevant for our studies. The 2D eigenfrequencies represent the cut-off (cut-on) frequencies of the corresponding 3D modes. The lowest axisymmetric eigenfrequency is thus the cut-off frequency of the $\alpha 1$ -mode.

Figure 9. shows five eigenfrequencies as a function of the wall elastic modulus E . The curves are universal at constant SDR and do not depend on the particular pipe diameter. At very small elastic moduli E the eigenfrequency f_{eig} is proportional to \sqrt{E} (linear curve sections on the left of Fig. 9.). At intermediate E the eigenfrequency curves increase in steps as a function of the elastic modulus. Finally at large elastic moduli $E \gg B_w$ the eigenmodes correspond to Bessel functions, which are the analytical solutions of the Helmholtz equation (2) for sound hard boundary conditions (i.e. no displacement at pipe wall). The stationary values (zeros) of the Bessel function $J_l(x)$ are indicated on the right of Fig. 9. They are in perfect agreement with the simulated values. It is clear from Fig. 9. that the fundamental $\alpha 1$ mode in iron pipes ($E = 200$ GPa) is different from that in polyethylene pipes ($E = 2$ GPa), where the pipe wall contributes an important fraction to the sound wave propagation.

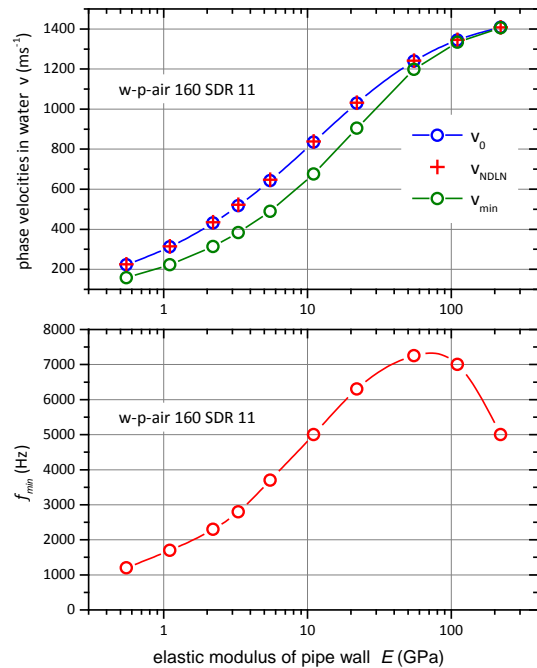


Figure 8. Top graph: characteristic phase velocities as a function of pipe wall elasticity. v_0 is the velocity at very low frequency. v_{min} is the minimum velocity and v_{NDLN} is obtained by Eq. (5). Lower graph: frequency of minimum phase velocity as a function of wall elasticity. The data are extracted from figure 6.

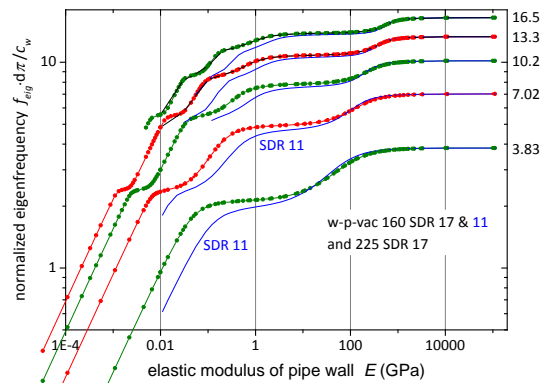


Figure 9. Eigenfrequencies as a function of pipe wall elasticity. The eigenfrequencies are normalized according to Eq. (4). The green and red curves are for SDR = 17 and two different diameters. The blue lines are for SDR = 11 and 160 mm outer diameter. Note that the values of the outer diameter (160 mm or 225 mm) are not relevant, as long as the SDR is constant (scalability, see text).

5. Conclusions

We investigated the propagation of the acoustic α_1 -mode in polyethylene pipes. This is the fundamental axisymmetric mode of the water column in the pipe at low frequency. Universal dispersion relations of the α_1 mode were obtained as a function of the standard dimension ratio SDR and of the material surrounding the pipe (soil, air). We found that at low frequency there exists little dispersion and that the “DC” phase velocity v_0 of the leak noise is independent of the surrounding material.

The evolution of the dispersion curves with increasing elastic modulus E of the pipe layer was presented. Simulated curves for $E = 2.2$ GPa showed perfect agreement with experimental data.

The 2D eigenfrequencies (equal to 3D cut-off/cut-on frequencies) increase in steps with increasing pipe wall elasticity, matching the analytical values in the limit of hard walls.

Investigation of the reflection of the acoustic α_1 -mode at bends or T-joints is feasible by the present simulation method, if the appropriate modal decomposition technique is employed (see e.g. Ref. [14]). The topic of bends and joints has already been approached by others [15, 16].

6. References

1. Hinni AG, Gewerbestrasse 18, CH-4105 Biel-Benken, Switzerland <http://www.hinni.ch/> (last visited 28.7.2014)
2. System *Lorno* www.hinni.ch/index.php?option=com_content&view=article&id=108&Itemid=19&lang=en (last visited 28.7.2014)
3. H.V. Fuchs and R. Riehle, Ten Years of Experience with Leak Detection by Acoustic Signal Analysis, *Applied Acoustics*, **33**, 1-19 (1991)
4. Y. Gao, M.J. Brennan, P.F. Joseph, J.M. Muggleton and O. Hunaidi, A Model of the Correlation Function of Leak Noise in Buried Plastic Pipes, *Journal of Sound and Vibration*, **277**, 133-148 (2004) <http://dx.doi.org/10.1016/j.jsv.2003.08.045>

5. Y. Gao, M.J. Brennan and P.F. Joseph, A comparison of time delay estimators for the detection of leak noise signals in plastic water distribution pipes, *Journal of Sound and Vibration*, **292**, 552-570 (2006)
6. R. Long, P. Cawley and M. Lowe, Acoustic wave propagation in buried iron water pipes, *Proc. R. Soc. Lond. A*, **459**, 2749-2770 (2003)
7. R. Long, M. Lowe and P. Cawley, Attenuation characteristics of the fundamental modes that propagate in buried iron water pipes, *Ultrasonics*, **41**, 509-519 (2003)
8. J.M. Muggleton, M.J. Brennan, R.J. Pinnington and Y. Gao, A novel sensor for measuring the acoustic pressure in buried plastic water pipes, *Journal of Sound and Vibration*, **295**, 1085-1098 (2006) <http://dx.doi.org/10.1016/j.jsv.2006.01.032>
9. K. Baik, J. Jiang and T.G. Leighton, Acoustic attenuation, phase and group velocities in liquid-filled pipes: Theory, experiment, and examples of water and mercury, *J. Acoust. Soc. Am.* **128**, 2610-2624 (2010)
10. COMSOL Multiphysics®, Version 4.4, <http://www.comsol.com/>
11. A.D. Pierce, *Basic Linear Acoustics*, Chapter 3 in *Springer Handbook of Acoustics*, Ed. T.D. Rossing, Springer, ISBN 978-0-387-30446-5
12. AGRU Kunststofftechnik GmbH Ing.-Pesendorfer-Str. 31, A-4540 Bad Hall, Österreich/Austria, <http://www.agru.at/> (last visited 28.7.2014)
13. www.mathworks.com, Version R2010b
14. T. Graf and J. Pan, *J. Acoust. Soc. Am.*, **134**, 292-299 (2013)
15. J.M. Muggleton, M.J. Brennan, R.J. Pinnington and Y. Gao, A novel sensor for measuring the acoustic pressure in buried plastic water pipes, *Journal of Sound and Vibration*, **295**, 1085-1098 (2006), <http://dx.doi.org/10.1016/j.jsv.2006.01.032>
16. A. Demma, B. Pavlakovic, P. Cawley and M. Lowe, The Effect of Bends on the Propagation of Guided Waves in Pipes, *J. Pressure Vessel Technol.*, **127**, 328-335 (2005)

7. Acknowledgements

We would like to thank Urs Riesen and Jules Graber from Hinni AG for helpful discussions and for initiating the present study. This work was partially supported by CTI Switzerland.